The life cycle of a monsoon season viewed from TRMM, GPM, CLOUDSAT and Reanalysis data sets

T. N. Krishnamurti and Dipak Sahu
Department of Earth, Ocean and Atmospheric Science,
Florida State University, Tallahassee, FL 32306

NASA PMM 2017 Science Team Meeting
October 16-20, 2017, San Diego, CA

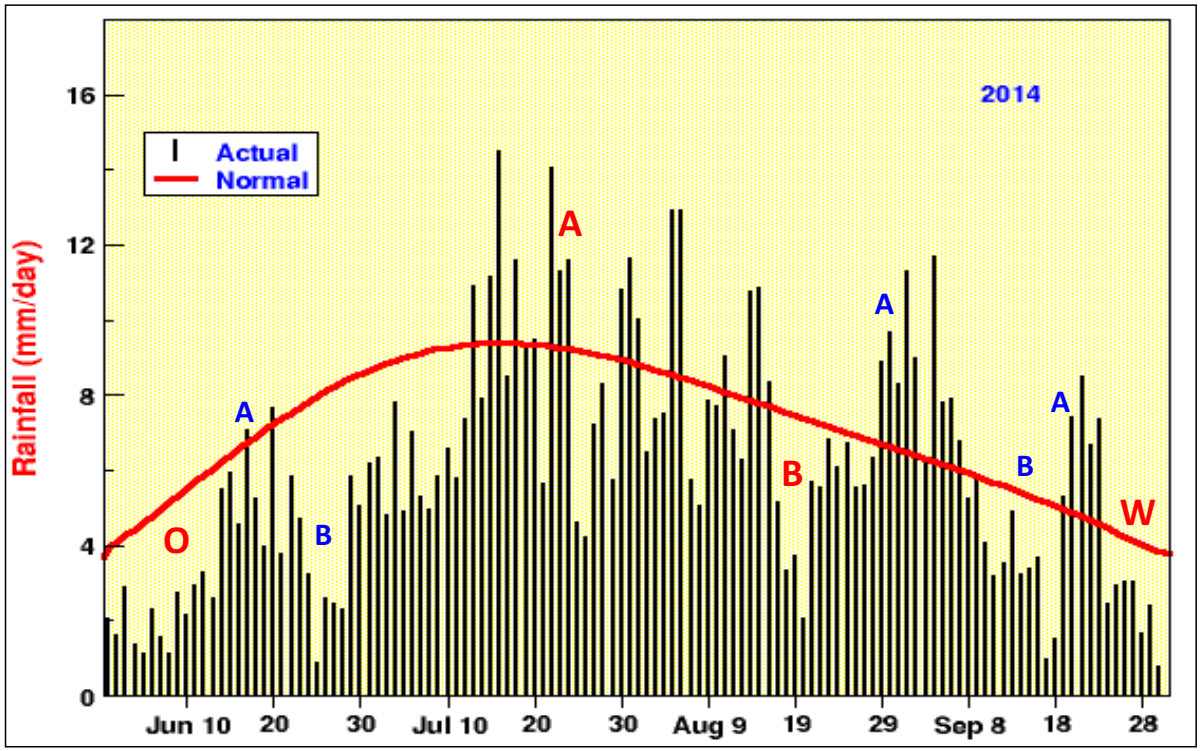

O → Onset

A → Active

B → Break

W → Withdrawal

Evolution of all-India daily area-weighted mean rainfall (mm/day) during the monsoon 2014. The onset (**O**), active (**A**), break (**B**), and withdrawal (**W**) phases are chosen based on the daily rainfall time series.

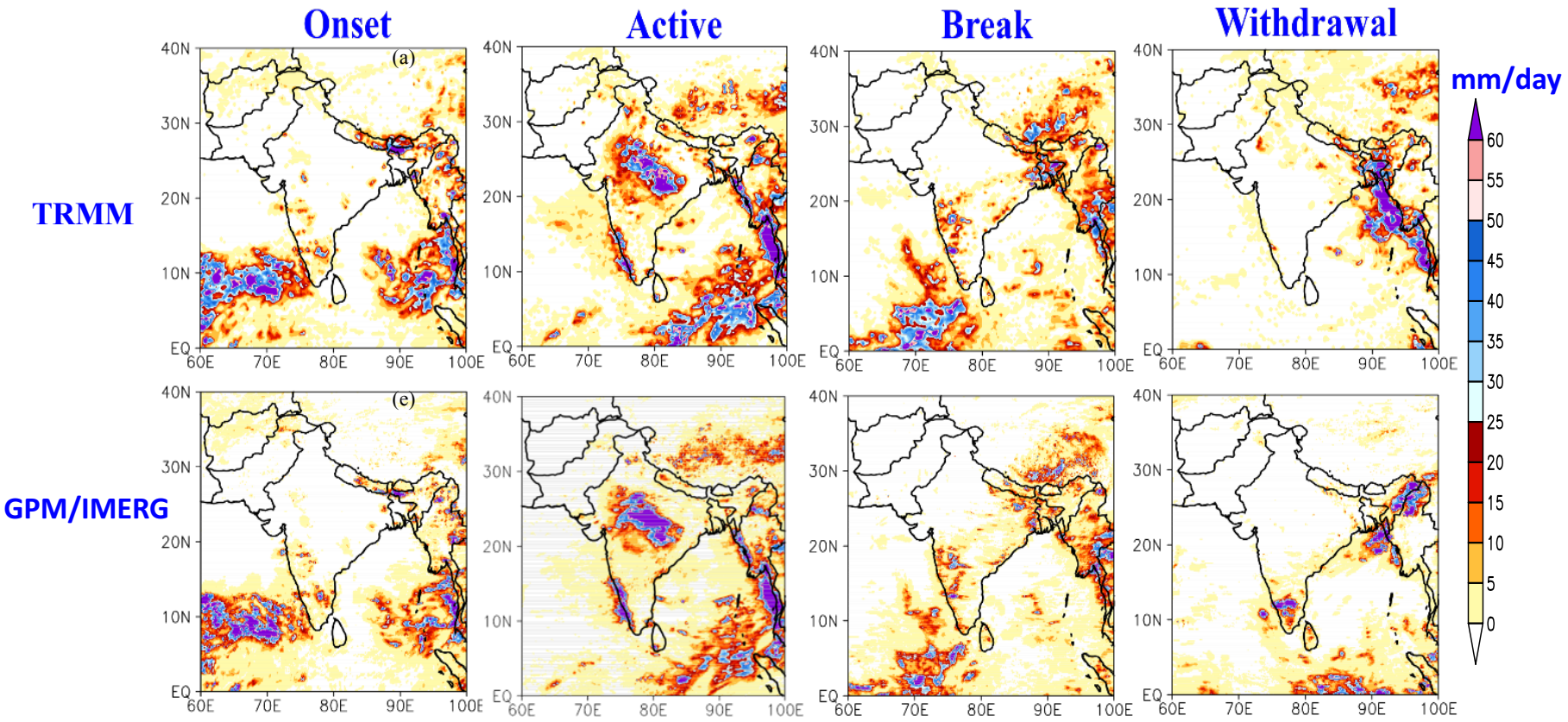

The TRMM (upper panel) and GPM/IMERG (lower panel) based rains (mm/day), for individual days, during the monsoon phases for 2014.

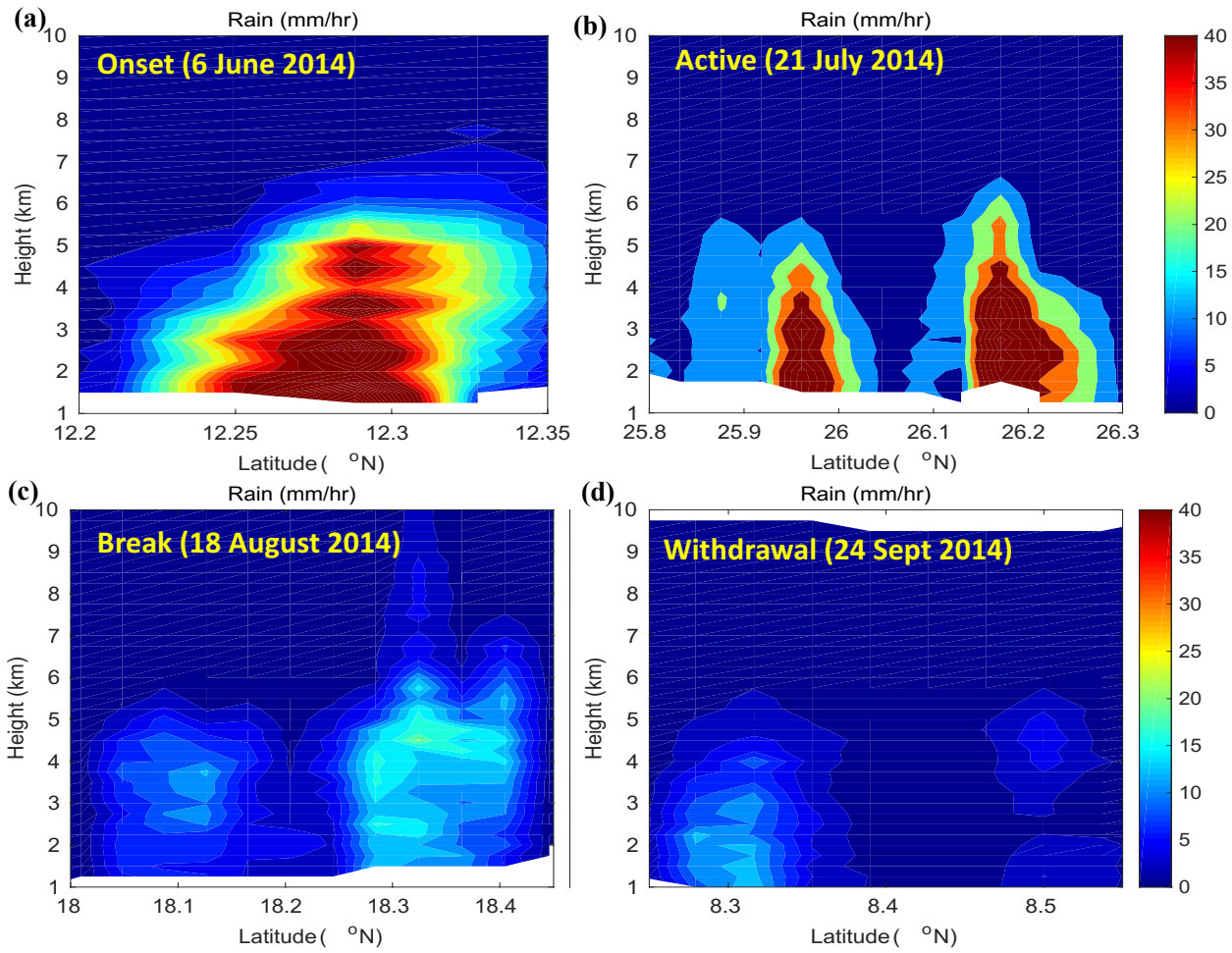

TRMM Radar Rain rate

Vertical structure of rain rate (mm/hr) from TRMM 2A25 PR data sets for selected satellite pass during (a) Onset (06 June 2014), (b) Active (21 July 2014), (b) Break (18 August 2014) and (d) Withdrawal (24 September 2014) phases of monsoon 2014.

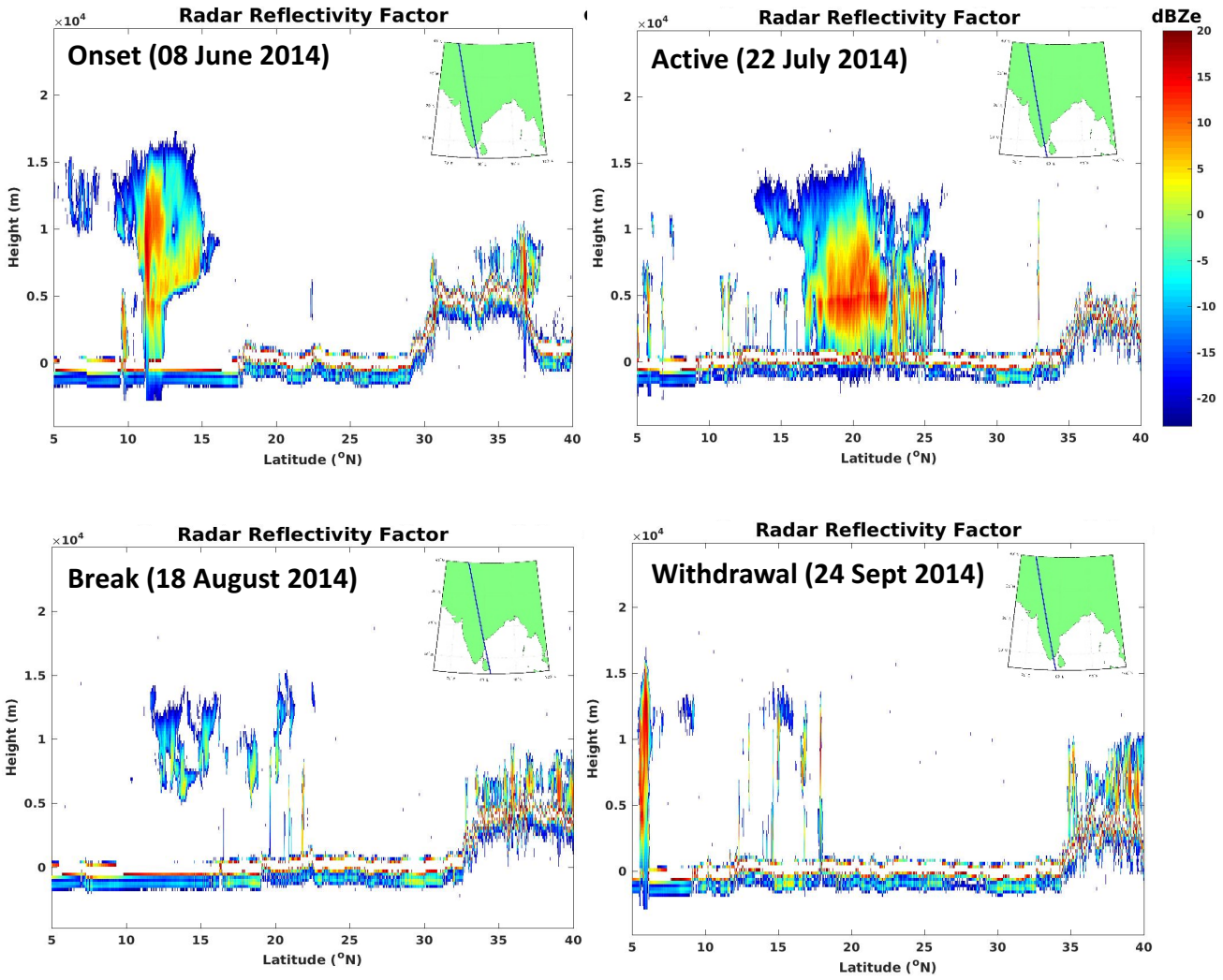

CLOUDSAT Radar Reflectivity

The **2B-GEOPROF** radar reflectivity from CLOUDSAT satellite measurement along the satellite track passes over Indian landmass (inset) during the (a) **Onset** (8 June 2014: Granule No.: 43153), (b) **Active** (22 July 2014: Granule No. 43794), (c) **Break** (18 August 2014: Granule No. 44187), and (d) **Withdrawal** (24 September 2014: Granule No. 44726).

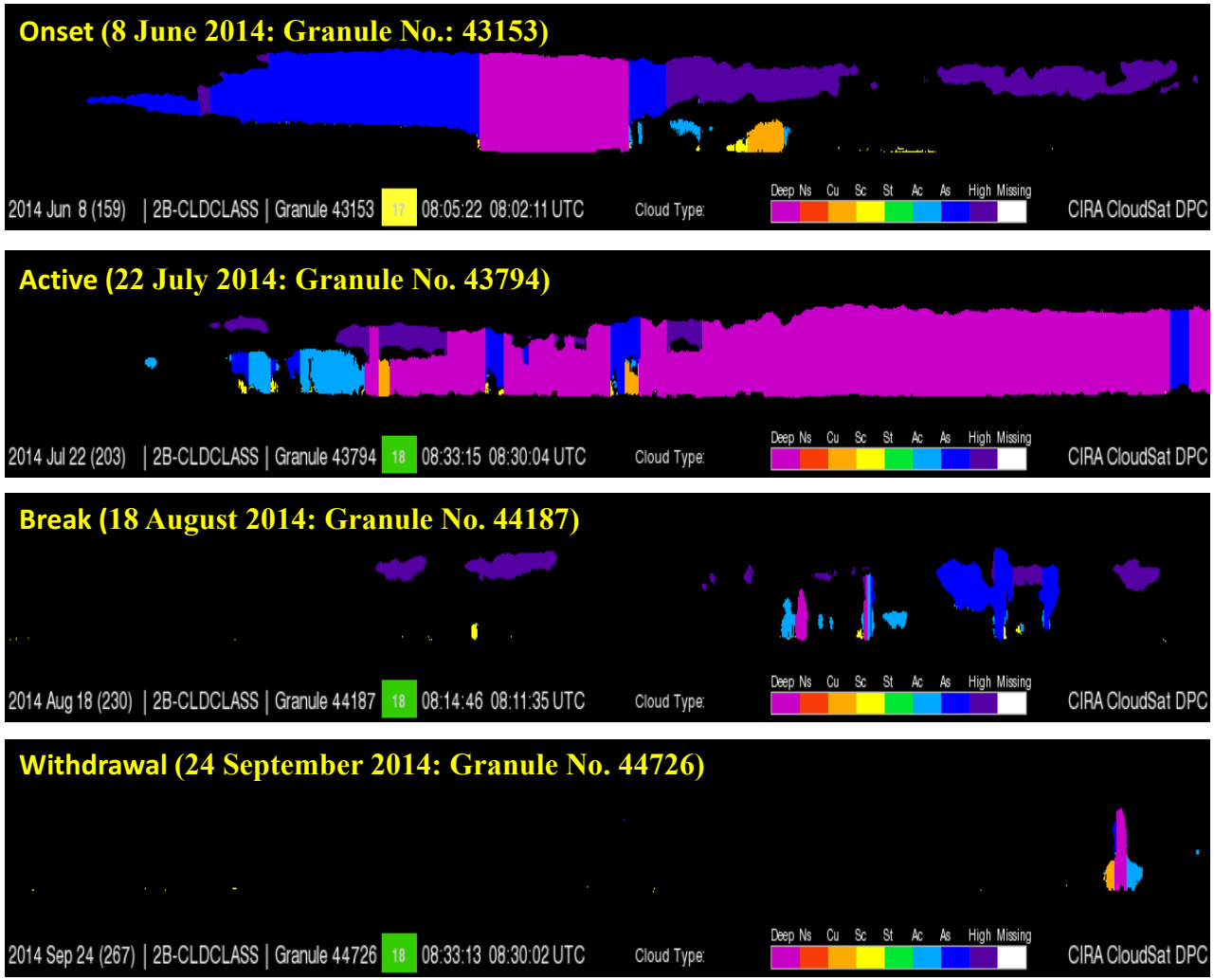

CLOUDSAT Cloud Classification

The cloud classifications from **2B-CLDCLASS** data product from CLOUDSAT satellite measurements during the (a) onset (8 June 2014: **Granule No.: 43153**), (b) active (22 July 2014: **Granule No. 43794**), (c) break (18 August 2014: **Granule No. 44187**), and (d) withdrawal (24 September 2014: **Granule No. 44726**). The segments are selected from the corresponding satellite orbital tracks as shown in the previous figure for 2B-GEOPROF radar reflectivity. The segment-18 (Lat: 17.1-28.6) and segment-17 (Lat: 5.5-17.1) are chosen based on their geographical pass over Indian landmass.

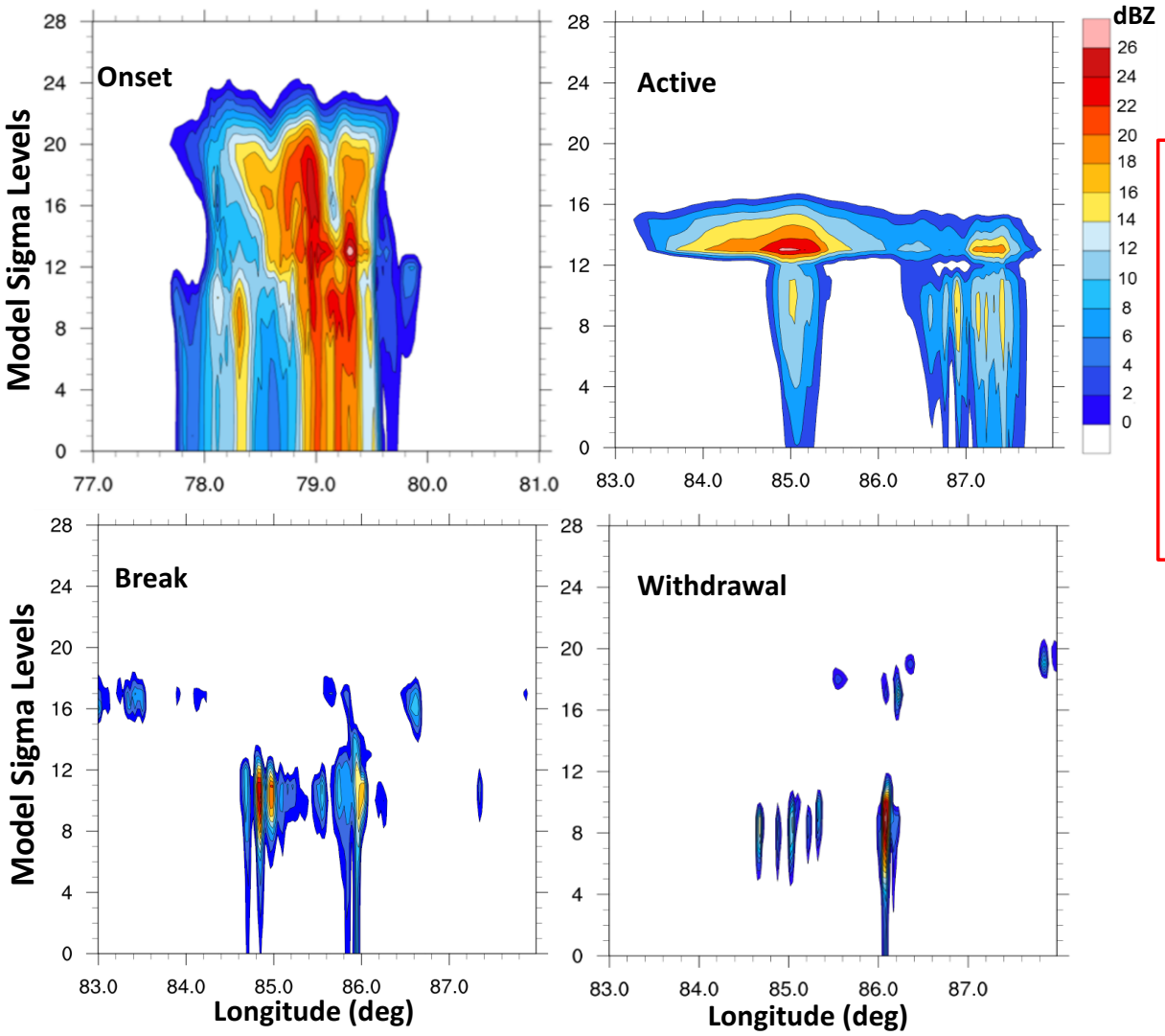

WRF Radar Reflectivity

Vertical structures of radar reflectivity (dBZ) for selected individual days derived from cloud resolving model (WRF) simulation during (a) Onset (10 June 2014), (b) Active (22 July 2014), (c) Break (18 August 2014) and (c) Withdrawal (24 Sept 2014) phases of monsoon 2014. The Y-axis show model sigma levels and X-axis show Longitude in degree East.

WRF Hydrometeors over Central India

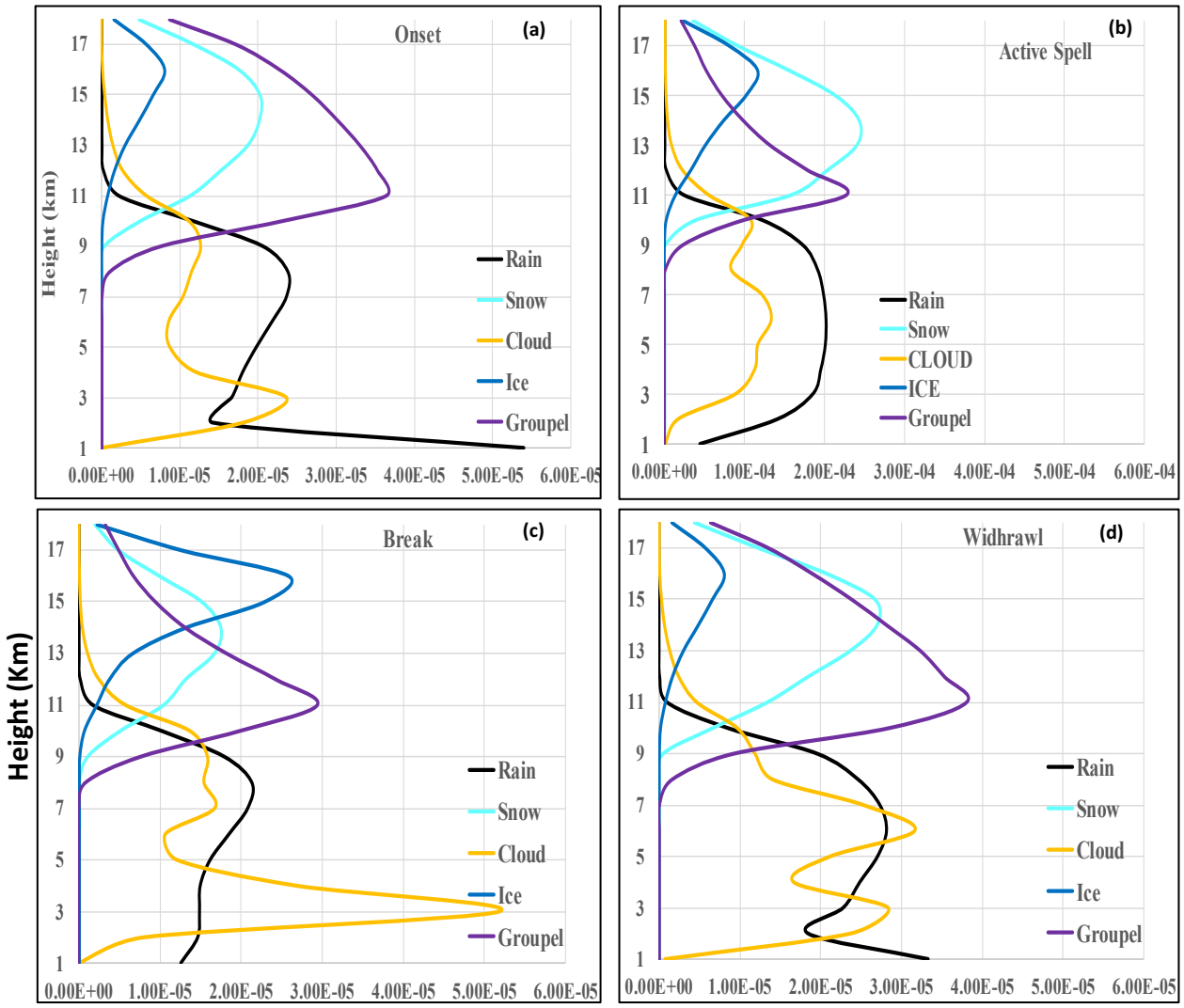

Vertical profiles of domain averaged (Central India: 20-27.5 ^{o}N and 75-82.5 ^{o}E) mean rain, snow, cloud, ice and graupel during (a) Onset (6-10 June 2014), (b) Active (21-24 July 2014), (c) Break (17-20 August 2014) and (d) Withdrawal (24-29 September 2014) phases of summer monsoon 2014 season derived from cloud resolving model (WRF) simulations. The abscissas show mixing ratio with units Kg/Kg.

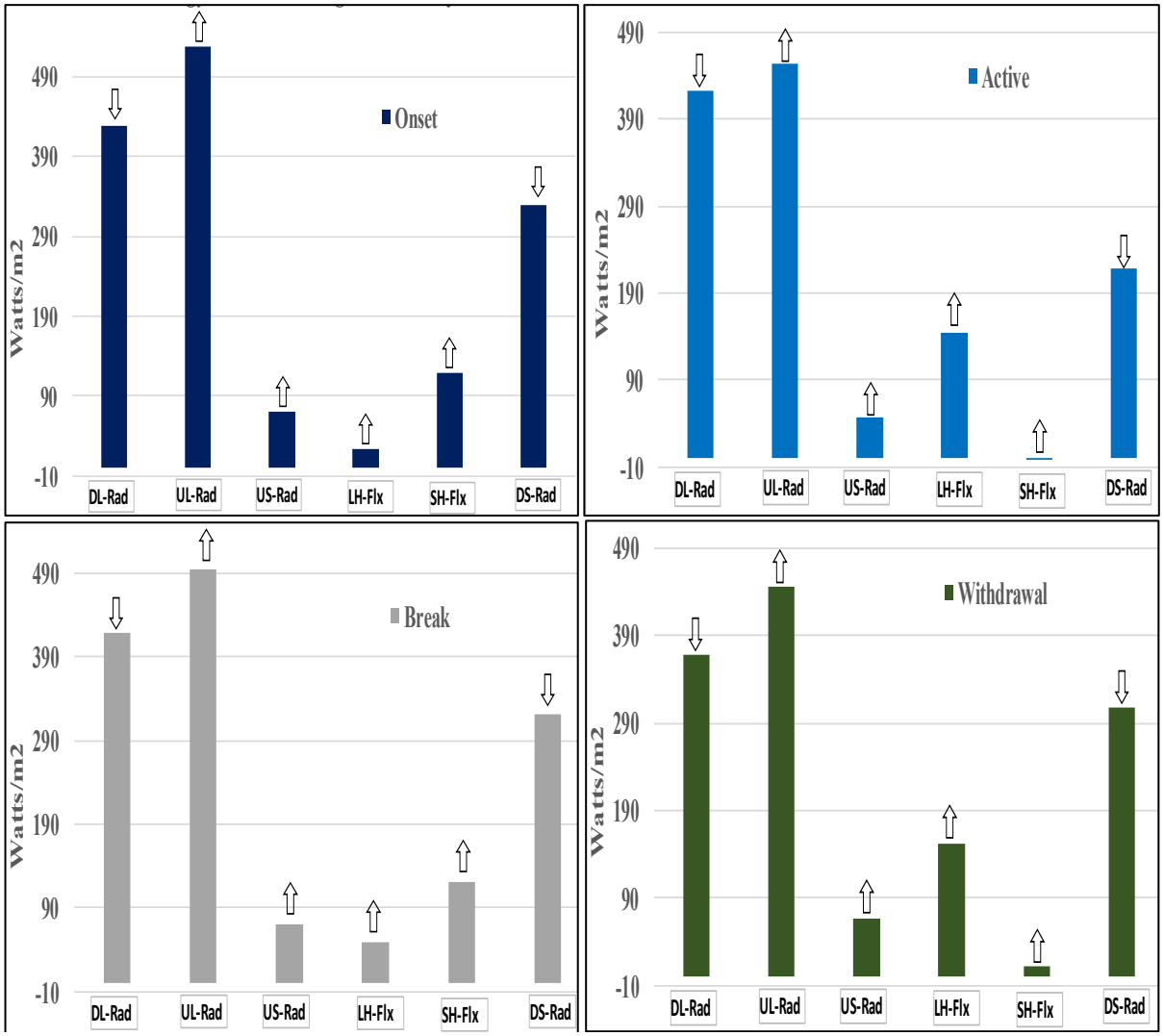

Mean Surface Energy Balance over Central India

Mean surface energy balance during the (a) Onset (06-10 June), (b) Active (21-24 July), (c) Break (17-20 August) and (d) Withdrawal (24-29 September) phases of monsoon 2014 derived from the cloud resolving model (WRF) simulation. All the variables are domain averaged over Central India (20-27.5 ^{o}N and 75-82.5 ^{o}E) and time mean of the respective phases.

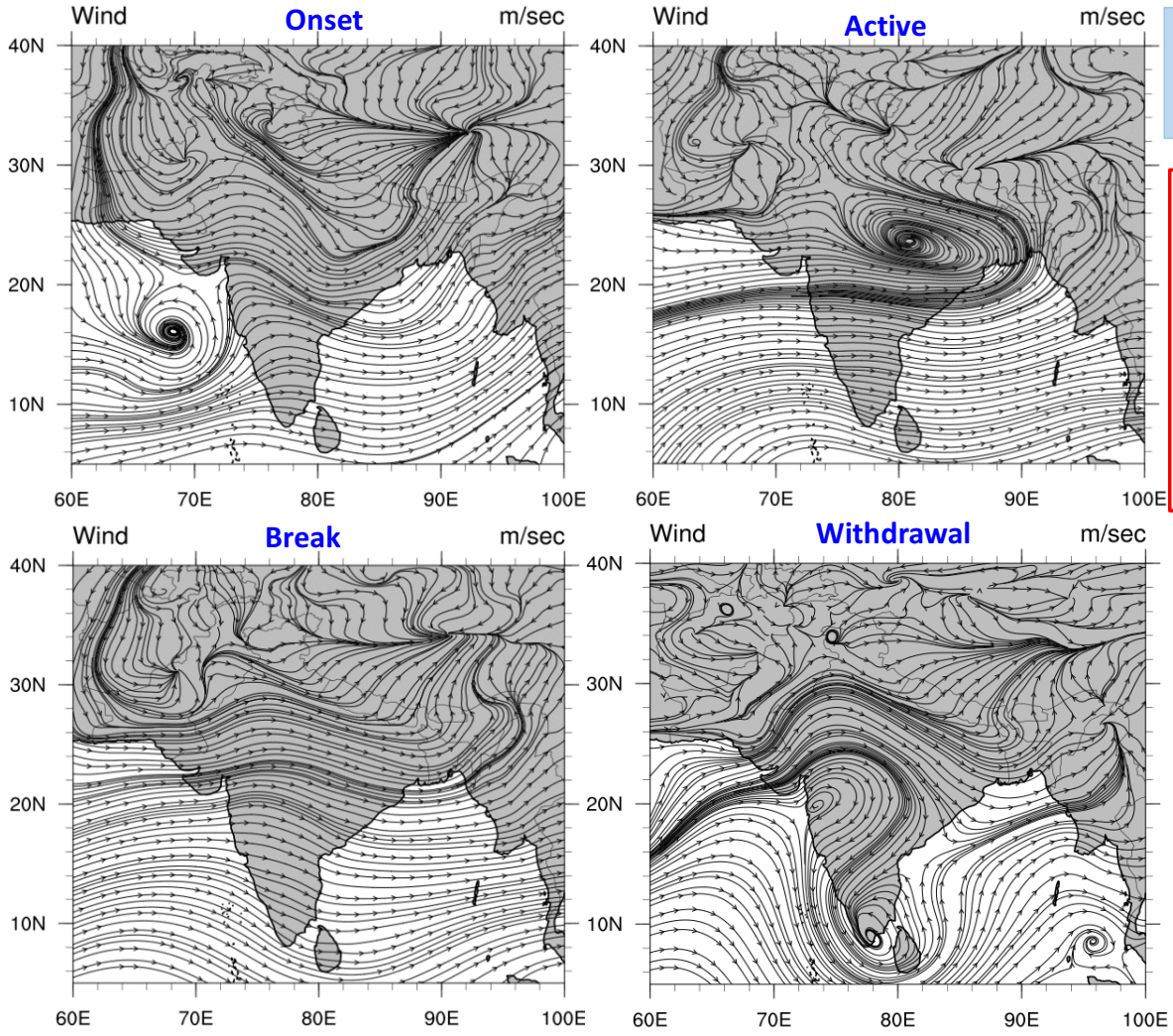

Mean wind streamlines at 850hPa from ERA_Interim

Spatial patterns of mean wind streamlines at 850hPa over Indian landmass during (a) Onset (6-10 June 2014), (b) Active phase (21-24 July 2014) (c) Break phase (17-20 August 2014), and (d) Withdrawal phase (24-29 sept 2014) of monsoon 2014 derived from ERA Interim data sets.

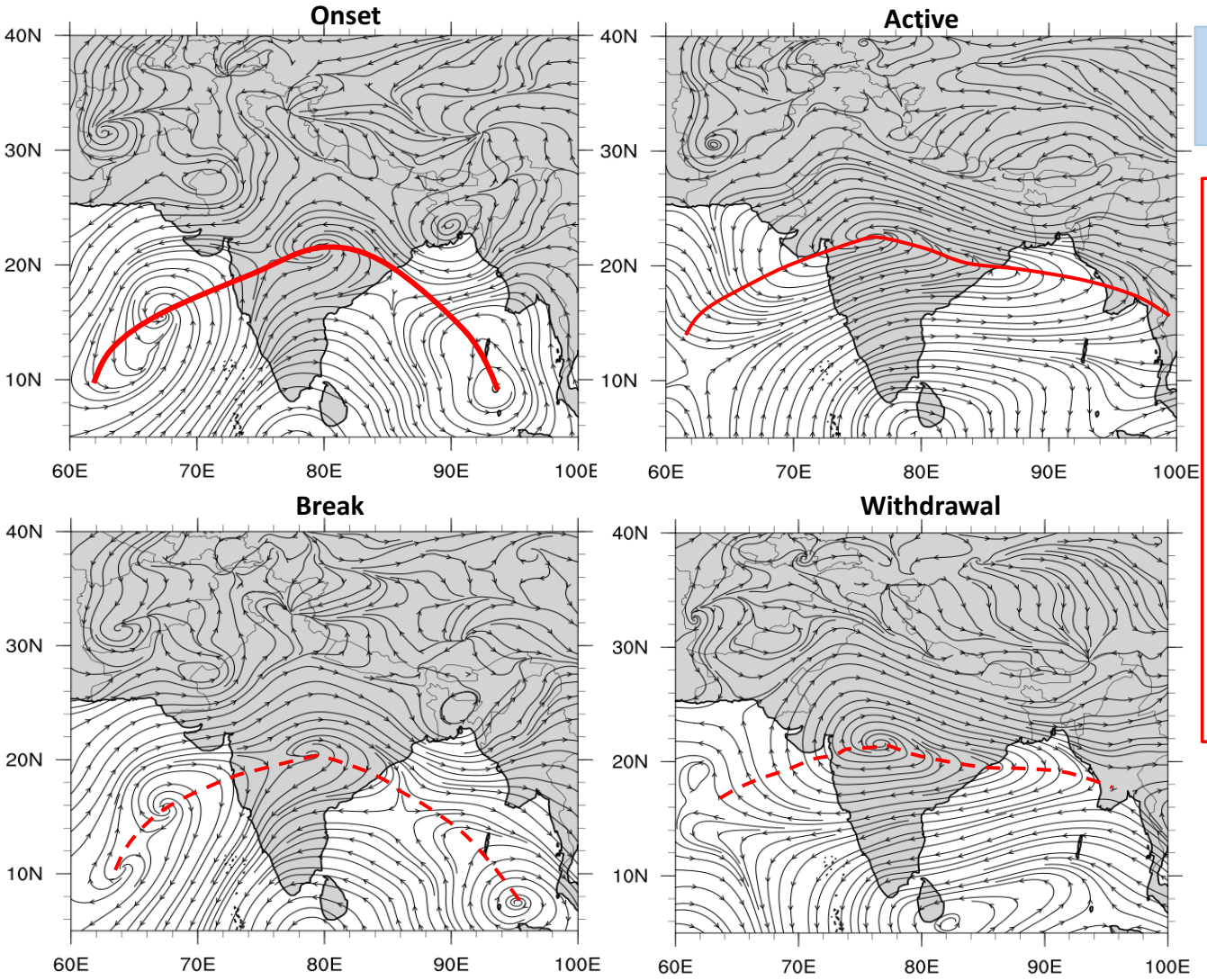

ISO (30-60 days) at 850hPa from ERA_Interim

Butterworth low pass filter (30-60 days) ISO streamline at 850hPa estimated from ERA Interim data sets during (a) Onset (06-10 June 2014), (b) Active (21-24 July 2014), (c) Break (17-20 August 2014) and (d) Withdrawal (24-29 September 2014) phases of Monsoon 2014. The solid red line marked the counterclockwise circulation of monsoon axis and dashed red line marked the clockwise circulation of monsoon axis.

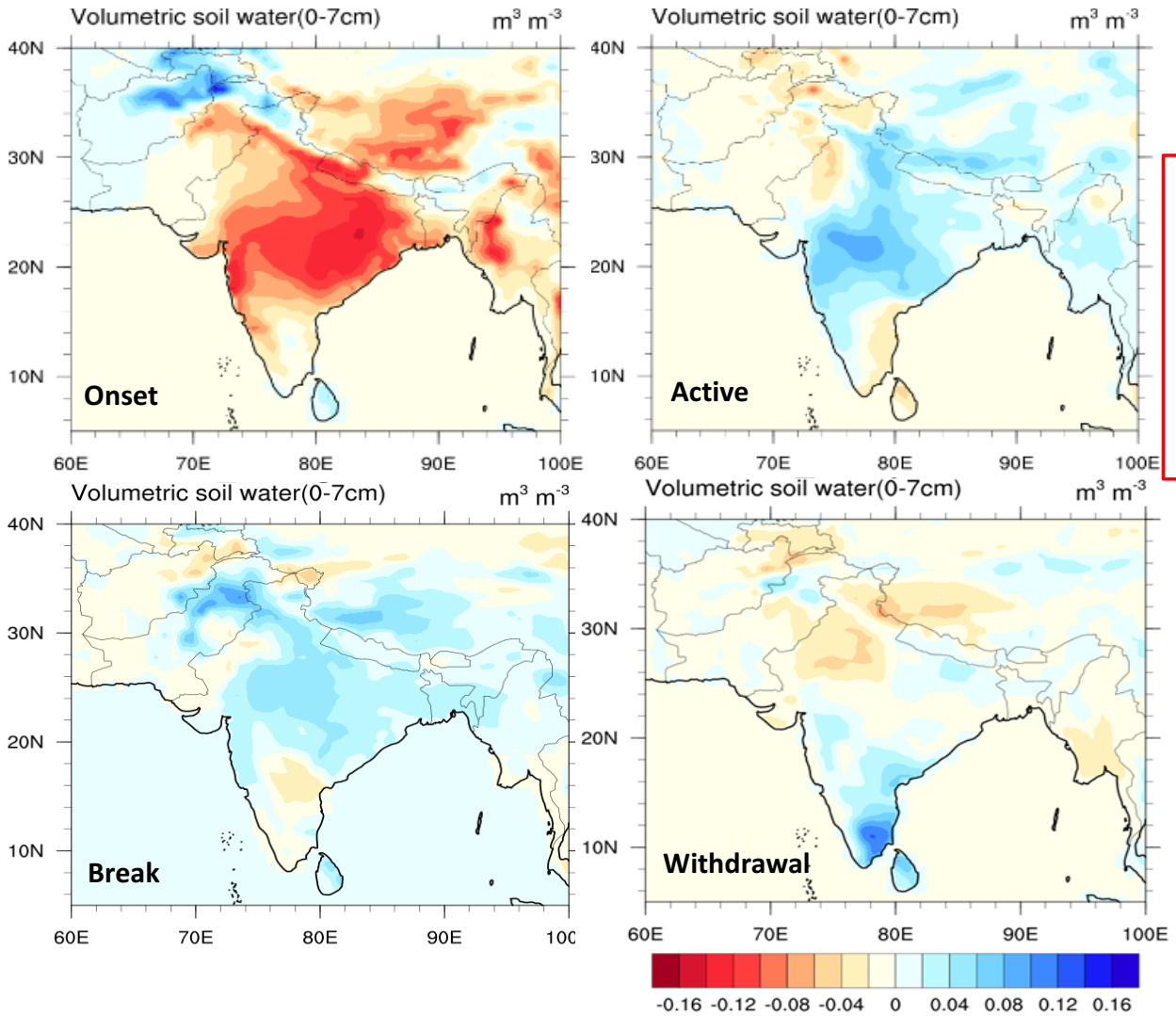

Soil Moisture Anomaly from ERA_Interim

Spatial distribution of soil moisture anomaly during (a) Onset (6-10 June), (b) Active (21-24 July), (c) Break (17-20 August) and (c) Withdrawal (24-29 September) phases of 2014 Indian summer monsoon derived from ERA Interim data sets.

- **Vertically integrated mean moisture flux (vector) and moisture convergence/divergence (+ve/-ve (kg/m.sec)) estimated during the phases of Monsoon:**

$M_x = -\frac{1}{g}\int_{Psuf}^{Ptop} U.q \ dp$, is the total column zonal flux of moisture

$M_y = -\frac{1}{g}\int_{Psuf}^{Ptop} V.q \ dp$, is the total column meridional flux of moisture

$M = i.M_x + j.M_y$, Representation of vertically integrated moisture transport vector

$MFC = (-1) * \nabla.M$, Convergence of vertically integrated moisture transport

Where g is the acceleration due to gravity, U is the zonal wind component, V is the meridional wind component, ∇ is the del operator, and q is the moisture parameter.

vertically integrated mean moisture flux (vector) and moisture convergence

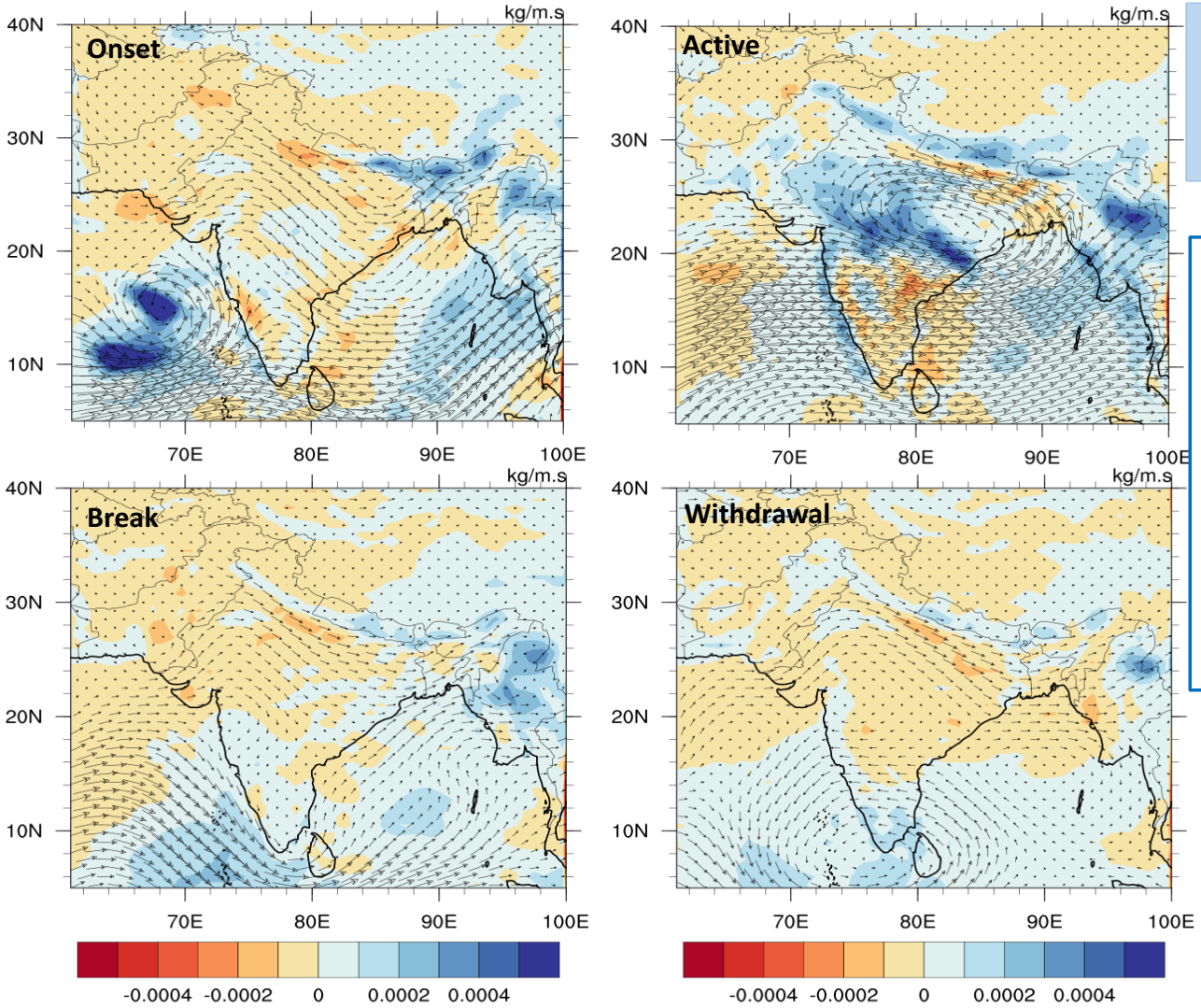

Spatial distribution of vertically integrated mean moisture flux (vector) and moisture convergence/divergence (+ve/-ve (kg/m.sec): shaded) during (a) Onset phase (6-10 June), (b) Active phase (21-24 July), (c) Break phase (17-20 August) and (c) Withdrawal phase (24-29 September) of 2014 Indian summer monsoon derived from ERA Interim data sets.

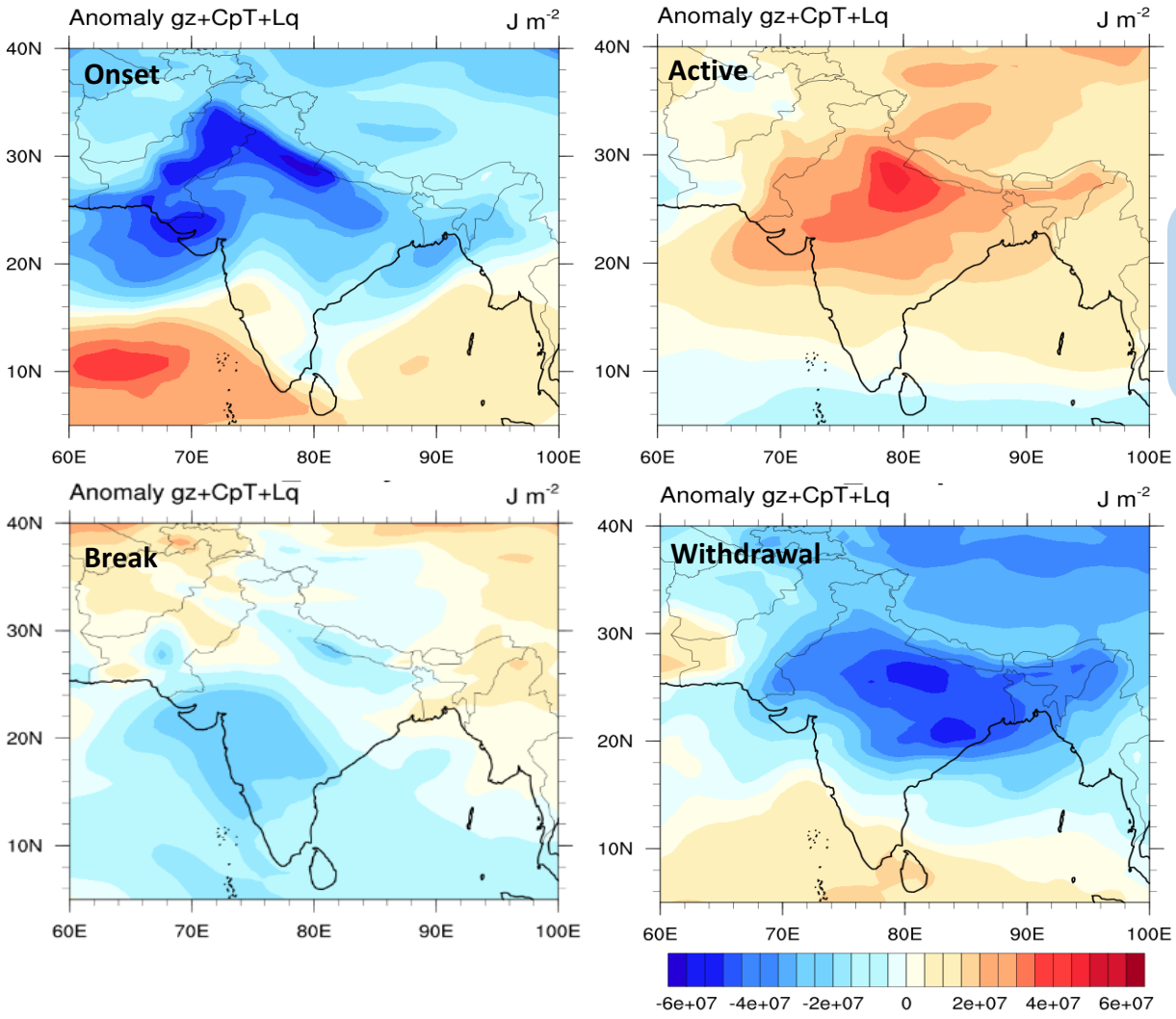

Vertically Integrated Moist Static Energy Anomaly from ERA_Interim

Vertically Integrated Moist Static Energy

$$= \frac{1}{g}\int_{P_{sf}}^{P_{top}} \left(gZ + C_pT + Lq\right) dp$$

Spatial distribution of vertically integrated moist static energy ($gZ+C_pT+Lq$) anomaly during (a) Onset phase (6-10 June) (b) Active phase (21-24 July), (c) Break phase (17-20 August) and (d) Withdrawal phase (24-29 September) of 2014 Indian summer monsoon.

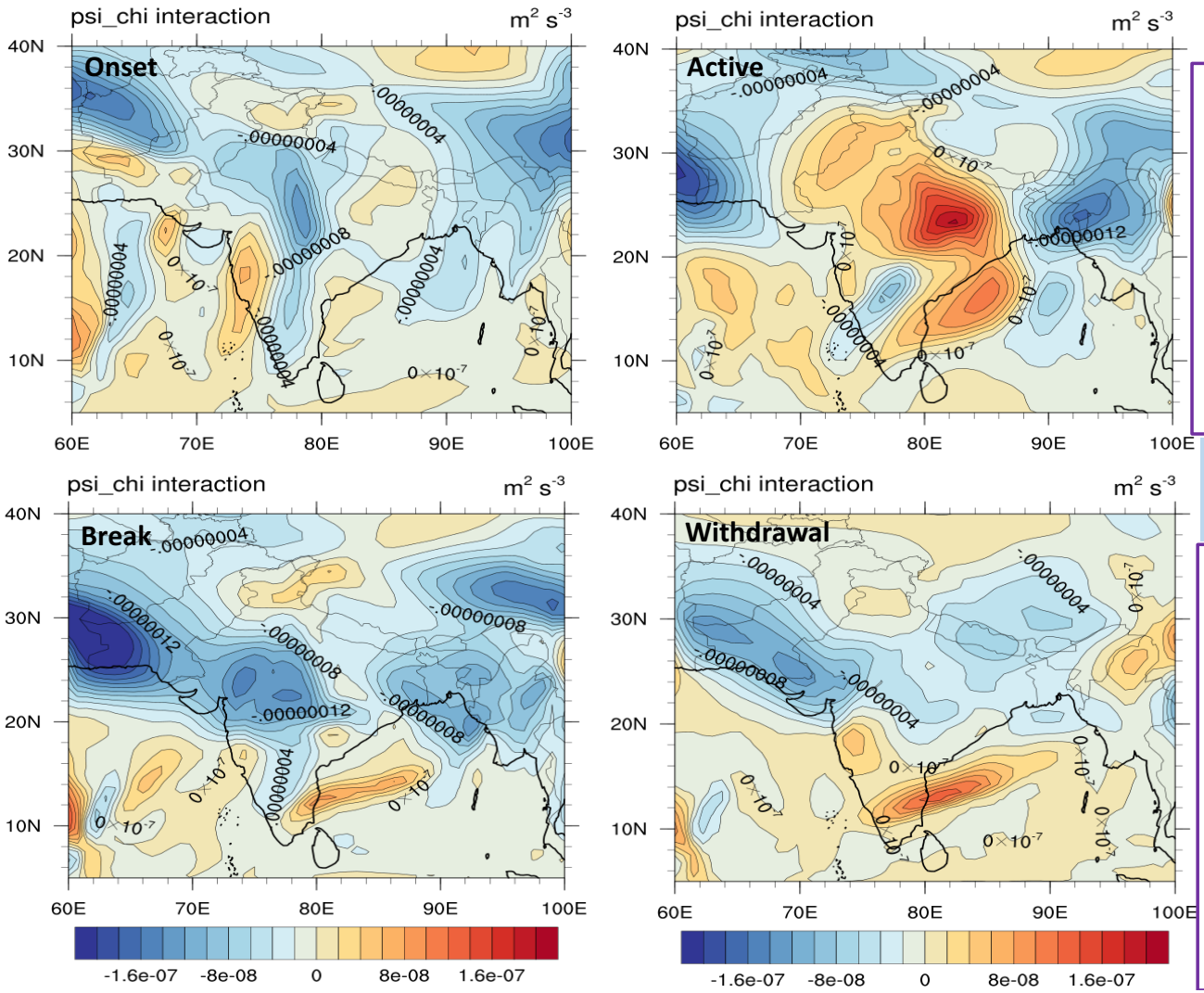

Psi-Chi Interaction

Mean $(f\overline{\overline{\nabla\psi.\nabla\chi}} + \overline{\overline{\nabla^2\psi\nabla\psi.\nabla\chi}})$ from ψ-χ interactions during (a) **Onset** phase (6-10 June), (b) **Active** phase (21-24 July) (c) **Break** phase (17-20 August), and (d) **Withdrawal** phase (22-26 September) of 2014 Indian summer monsoon derived from ERA Interim data sets.

Term1 $= f\overline{\overline{\nabla\psi.\nabla\chi}}$ **and**
Term2 $= \overline{\overline{\zeta\nabla\psi.\nabla\chi}}$ **where** $\zeta = \nabla^2\psi$,

Derived from the energy equations $\frac{\partial}{\partial t}K_\psi$ (**Krishnamurti et. al., 2006**) and given by,

$$\frac{\partial}{\partial t}\overline{\overline{K_\psi}} = \left[f\overline{\overline{\nabla\psi.\nabla\chi}} + \overline{\overline{\zeta\nabla\psi.\nabla\chi}} + \overline{\overline{\nabla^2\chi\frac{(\nabla\psi)^2}{2}}} + \overline{\overline{\omega J\left(\psi,\frac{\partial\chi}{\partial p}\right)}}\right] + \overline{\overline{F_\psi}}$$

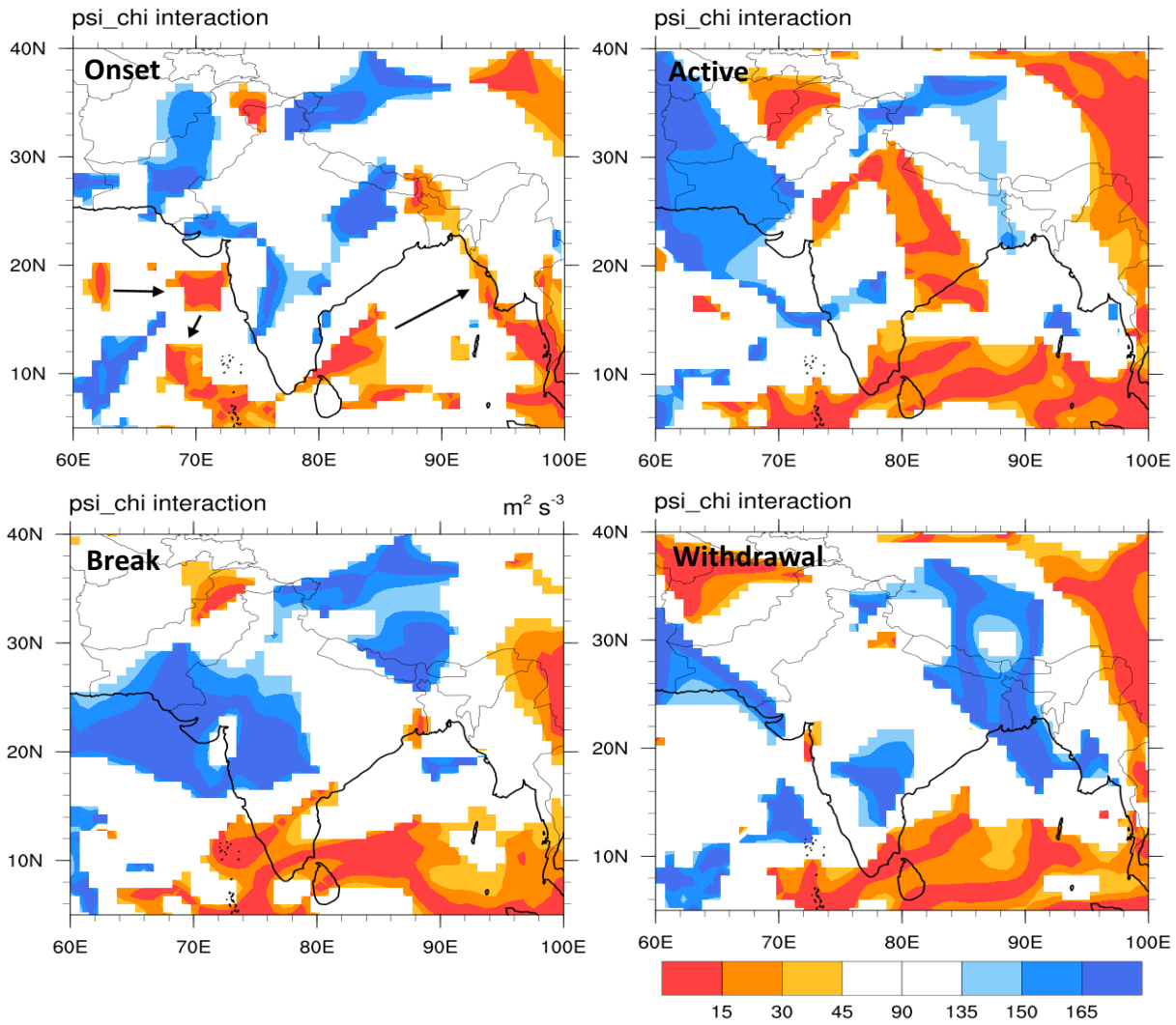

Psi-Chi Interaction

Mean angle **(x)** between $\nabla\psi$ **and** $\nabla\chi$ **vectors** during the (a) **Onset** (6-10 June), (b) **Active** phase (21-24 July) (c) **Break** phase (17-20 August), and (d) **Withdrawal** phase (24-29 September) of monsoon 2014 derived from ERA Interim data sets.

- The **Reddish color shows where** $0 \leq x \leq 45$, which represents the energy exchange from divergence to rotational kinetic energy.
- The **Bluish color shows where** $135 \leq x \leq 180$, which represents the rotational kinetic energy losing energy to divergent energy.

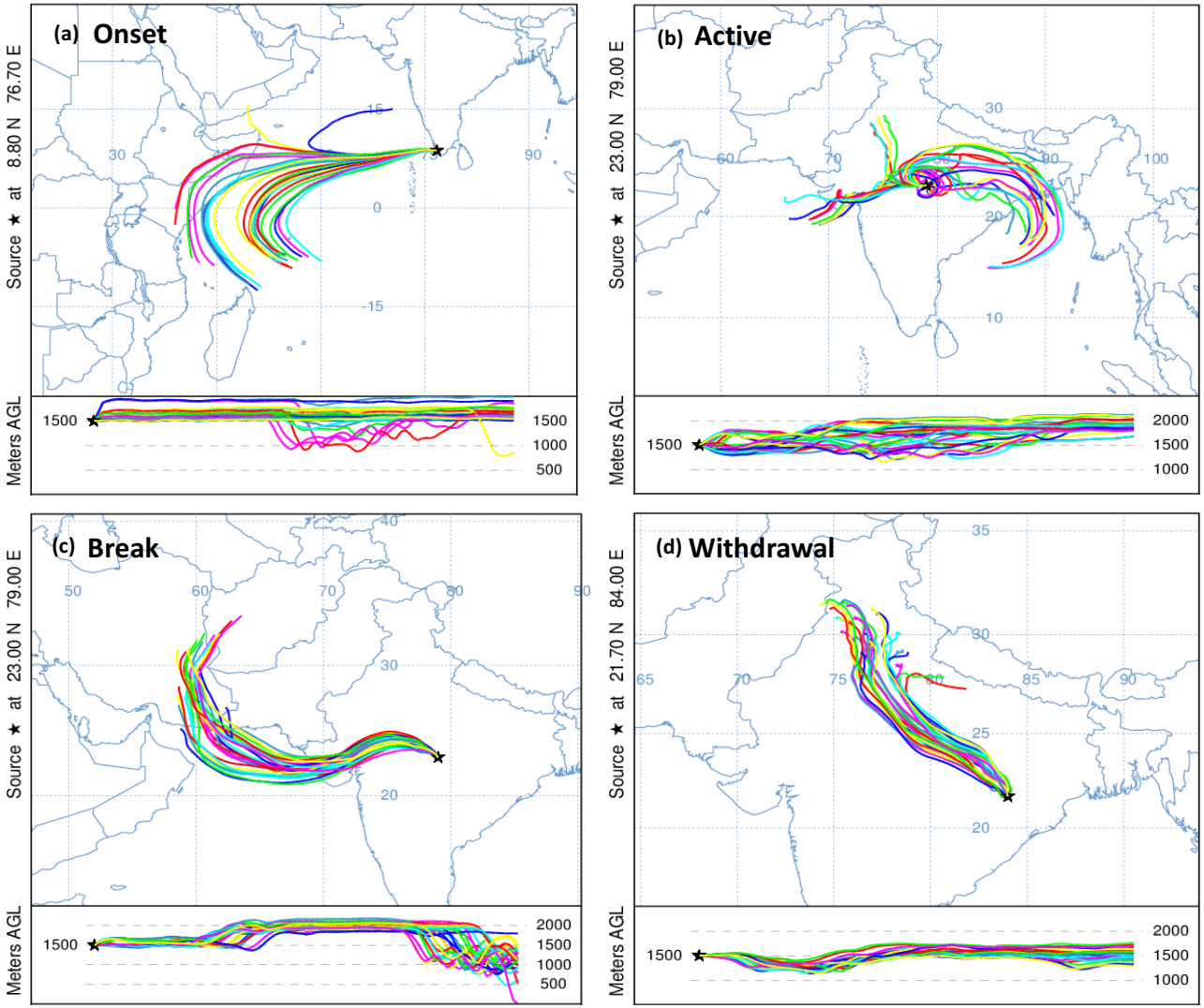

Monsoon Back Trajectories

Four-day back trajectories for selected days during the (a) Onset (10 June 2014), (b) Active (24 July 2014) (c) Break (18 August 2014), and (d) Withdrawal (24 sept 2014) phases of monsoon 2014 derived from GFS data (0.5º horizontal resolution).

Summary:

- **Through TRMM, GPM, CLOUDSAT observations and reanalysis products we found that during Monsoon phase transitions deep cumulonimbus clouds prevail whereas in the active monsoon phase the deep convective clouds and nimbostratus provides the steady heavy rains.**
- **The reanalysis products and modeling confirms the role of surface moisture flux, soil moisture and clouds modulating the surface energy balance during phase transitions.**
- **A large built up of positive values of moist static energy anomaly during the onset phase is located over northern India and foot-hills of the Himalayas, where extreme rain events are frequent.**
- **The evolution of the exchange of energy from divergent to the rotational kinetic energy (and vice-versa) has a robust role in the strengthening (or weakening) of the monsoon circulation.**

On-going work:

- **Why are these intraseasonal phases present? Active phase of MJO (time scale around 40 days, horizontal scale around 10,000 km) triggers ISO west of Sumatra island, this is a shear flow instability of the monsoon region in the presence of various phases of MJO. The scale of instability is on a horizontal scale of around 2500 km scale with the period of the MJO. That instability weakens over south east Asia and over Africa because of different wind shear environments.**
- **Numerical prediction of the above phase transitions are being modelled using physical initialization for precipitation and for soil moisture (using SMAP data sets).**

Thanks